N73-14709
NASA TM X-2679

NASA TECHNICAL MEMORANDUM

NASA TM X-2679

MULTIDIMENSIONAL ANALYSIS OF FAST-SPECTRUM MATERIAL REPLACEMENT MEASUREMENTS FOR SYSTEMATIC ESTIMATION OF CROSS-SECTION UNCERTAINTIES

by Paul G. Klann, Edward Lantz, and Wendell Mayo

Lewis Research Center
Cleveland, Ohio 44135

NATIONAL AERONAUTICS AND SPACE ADMINISTRATION • WASHINGTON, D. C. • JANUARY 1973

1. Report No.	2. Government Accession No.	3. Recipient's Catalog No.
NASA TM X-2679		

4. Title and Subtitle	5. Report Date
MULTIDIMENSIONAL ANALYSIS OF FAST-SPECTRUM MATERIAL REPLACEMENT MEASUREMENTS FOR SYSTEMATIC ESTIMATION OF CROSS-SECTION UNCERTAINTIES	January 1973
	6. Performing Organization Code

7. Author(s)	8. Performing Organization Report No.
Paul G. Klann, Edward Lantz, and Wendell Mayo	E-7069
	10. Work Unit No. 503-25

9. Performing Organization Name and Address	11. Contract or Grant No.
Lewis Research Center National Aeronautics and Space Administration Cleveland, Ohio 44135	

12. Sponsoring Agency Name and Address	13. Type of Report and Period Covered
National Aeronautics and Space Administration Washington, D.C. 20546	Technical Memorandum
	14. Sponsoring Agency Code

15. Supplementary Notes

16. Abstract

A series of central core and core-reflector interface sample replacement experiments for 16 materials performed in the NASA heavy-metal-reflected, fast spectrum critical assembly (NCA) were analyzed in four and 13 groups using the GAM II cross-section set. The individual worths obtained by TDSN and DOT P_0S_4 multidimensional transport theory calculations showed significant differences from the experimental results. These were attributed to cross-section uncertainties in the GAM II cross sections. Simultaneous analysis of the measured and calculated sample worths permitted separation of the worths into capture and scattering components which systematically provided fast spectrum averaged correction factors to the magnitudes of the GAM II absorption and scattering cross sections. Several Los Alamos clean critical assemblies containing Oy, Ta, and Mo as well as one of the NCA compositions were reanalyzed using the corrected cross sections. In all cases the eigenvalues were significantly improved and were recomputed to within 1 percent of the experimental eigenvalue. A comparable procedure may be used for ENDF cross sections when these are available.

17. Key Words (Suggested by Author(s))	18. Distribution Statement
Fast spectrum nuclear reactor; Fast spectrum reactor integral measurements; Systematic fast cross section correction; Partition of total cross sections; Large sample worth analysis; Refractory metals cross sections	Unclassified - unlimited

19. Security Classif. (of this report)	20. Security Classif. (of this page)	21. No. of Pages	22. Price*
Unclassified	Unclassified	35	$3.00

* For sale by the National Technical Information Service, Springfield, Virginia 22151

MULTIDIMENSIONAL ANALYSIS OF FAST-SPECTRUM MATERIAL REPLACEMENT MEASUREMENTS FOR SYSTEMATIC ESTIMATION OF CROSS-SECTION UNCERTAINTIES

by Paul G. Klann, Edward Lantz, and Wendell Mayo

Lewis Research Center

SUMMARY

A series of central core and core-interface full-core-length material-replacement experiments were performed in the NASA heavy-metal-reflected, fast spectrum critical assembly (NCA). The measured integral worths were individually calculated in four and 13 groups using the two-dimensional TDSN and DOT transport theory programs. Significant discrepancies were observed that are attributed to cross-section uncertainties in the GAM II cross-section set. In order to interpret these differences, a method of Engle, Hanson, and Paxton, wherein the integral reactivity of samples at various radii are separated into absorption and scattering components, was extended to the cylindrical geometry, multigroup transport theory results. This procedure permitted calculation of average fast-spectrum correction factors to the GAM II absorption and scattering input cross sections. The extended method is useful for consistent interpretation of in-core material replacement reactivity measurements so as to adjust average values of absorption and scattering cross section for nonfissioning materials. It applies principally to a fast-neutron spectrum reactor having negligible neutron flux in the resolved resonance region.

Several Los Alamos clean critical assemblies containing oralloy, tantalum, and molybdenum as well as an NASA critical assembly were reanalyzed using the corrected group cross sections obtained. In all cases the resulting eigenvalues were improved and were within 1 percent of the experimental eigenvalue.

INTRODUCTION

A technique for checking the validity of cross section data on an overall basis for calculation of eigenvalue is to compare critical assembly integral worth measurements

of dilute samples of material with transport theory calculations using first-order perturbation analysis (ref. 1). The reactivity worth measurements are usually made by inserting thin samples of the material into the center of the core. The difference between measurement and calculation of the sample reactivity is then primarily due to inconsistencies in the absorption cross section of the material because of the central location of the sample. In some experiments additional off-center reactivity measurements have been made in the presence of flux gradients. For these experiments the difference between calculated (by eigenvalue difference methods) and measured reactivity worths also provide data on the scattering cross section. Moore, Sargis, and Cohen (ref. 1) reported an extensive series of measurements and calculations using the perturbation and eigenvalue difference methods in a critical assembly that simulated a thermionic reactor reflected by beryllium oxide.

Engle, Hansen, and Paxton (ref. 2) analyzed the reactivity contributions in the reactor critical experiments Topsy, Godiva, and Jezebel and separated the absorption effects that are predominant in the center of the core from the scattering effects that are most important at the edge of the core. They showed that the measured integral worth at various radii in these spherical fast cores can be partitioned into a linear combination of a spatially independent spectrum-averaged absorption component and a spatially independent scattering component.

The purpose of the present analysis is to extend the concept of a linear partition into absorption and scattering components to two-dimensional cylindrical geometries calculated by the multigroup-transport-theory discrete-ordinates methods. The concept is applied quantitatively to central and edge full-core-length integral material-worth measurements on massive samples to obtain fast-spectrum-averaged corrections to the absorption and scattering components of the material cross sections. It is shown that these fast-spectrum-averaged correction factors are of the correct sign and magnitude to reduce the overpredictions in eigenvalue obtained with the GAM II (ref. 3) cross-section set previously used for the precritical calculations (ref. 4) for the heavy-metal-reflected, fast-spectrum critical assembly (ref. 5). The present material integral-worth measurements were carried out in this assembly.

MEASUREMENTS

The integral reactivity worths of 16 materials inserted as full-core-length samples of fuel, structure, and reflector materials of importance in the design of compact, fast spectrum, liquid-metal-cooled, high-temperature reactors were measured. The samples were inserted successively on the six outermost peripheral fuel-element positions and in the seven central positions of the NCA composition 5 critical assembly (ref. 5) as

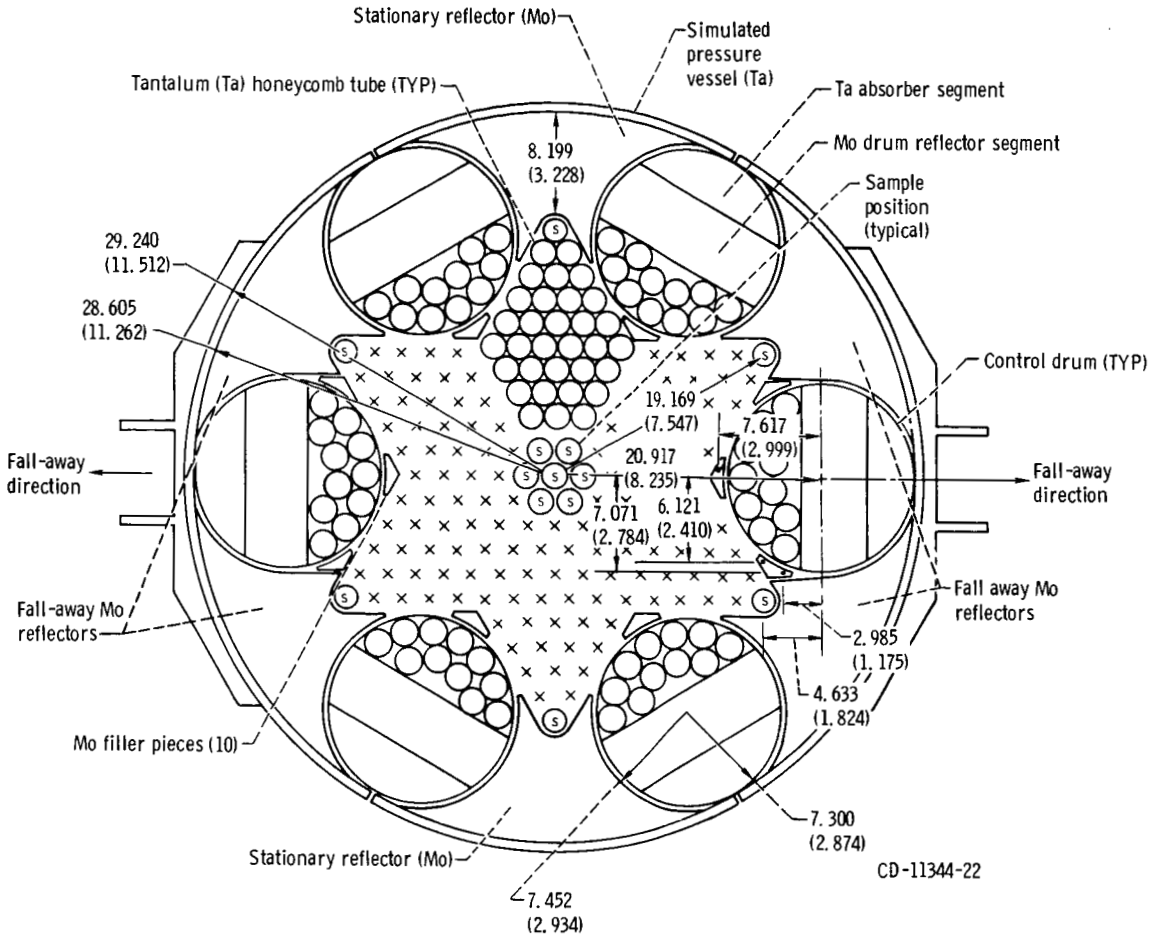

Figure 1. - Cross sectional view of critical assembly at core midplane. (All dimensions are in centimeters (in.).)

shown in figure 1. The samples were large (1.3 cm diam by about 37.5 cm long) and occupied the space normally filled with fuel rods in these elements. The large sample dimensions were selected in order to obtain relatively large values for the integral worths for the scattering materials, which have small intrinsic reactivity worth. A listing of the materials measured is given in tables I and II. The reactivity measurements were made by exchanging the sample to be measured with a reference sample (void) while the reactor was near critical. A remote sample changer was used and the flux-time profile was analyzed by the inverse kinetics technique. The measured values and the specific worth in millicents per gram are listed in tables I and II.

In order to obtain data on the effects of sample self-shielding, nine nearly dilute absorbers were measured at the center of the core using a reactivity oscillator and analysing the power oscillations by means of an iterative inverse kinetics program. The measured values are given in table III.

TABLE I. - COMPARISON OF CALCULATED AND MEASURED INTEGRAL

SAMPLE WORTHS AT SIX EDGE CORE LOCATIONS

[1.3-cm-diam by 37.5-cm-long samples.]

Material, m	Measured		Calculated			
			Four group		13 group	
	Worth, ¢	Specific worth, m¢/g	Worth, ¢	Specific worth, m¢/g	Worth, ¢	Specific worth, m¢/g
Li	4.36±0.07	27.00±0.43	[a]3.3±0.2	[a]20.6	[a]3.2±0.2	[a]19.7
^{6}Li(94.72%) ^{7}Li(5.20%)	-38.83±0.03	-307.87±2.49	-36.1±1 [b]-37.0±0.2 -41.2±0.2	-286.5 [b]-293.6 [c]-326.9	-38.9±0.2	-308.7
^{7}Li(99.993%) ^{6}Li(0.007%)	7.97±0.07	54.71±0.49	[a]7.0±0.2	[a]48.3	[a]6.3±0.2	[a]43.5
$^{7}Li_3N$(95.62%) $^{7}Li_2O$(1.82%) $^{7}LiOH$(2.56%)	10.36±0.09	43.351±0.38	[a]8.4±0.2	[a]35.4	----------	--------
Be	35.01±0.32	62.64±0.64	33.2±1	59.01	----------	--------
BeO	38.82±0.36	44.35±0.41	40.6±1	46.34	----------	--------
^{10}B(86.49%) ^{11}B(7.51%) C(2.46%) O(0.95%) H_2O(0.05%)	-83.151±0.88	-255.724±3.01	-55.6±0.2 [c]-59.7±0.2	-171.1 [c]-183.6	[c]-57.6±0.2	[c]-176.9
C	23.44±0.21	45.26±0.40	23.2±1 [c]23.6±0.2	44.82 [c]45.43	[c]22.8±0.2	[c]43.95
Nb-1%Zr	22.611±0.20	9.286±0.08	[c]24.0±0.2	[c]9.845	----------	--------
Mo	27.82±0.25	8.99±0.08	25.3±1 [c]29.2±1	8.160 [c]9.411	[c]28.6±0.2	[c]9.196
Hf	11.35±0.10	2.96±0.03	16.3±0.2 16.3±1 [c]16.4±0.2	4.121 4.121 [c]4.146	[c]16.77±0.2	[c]4.238
Ta	10.10±0.08	2.01±0.02	12.7±0.2 13.2±1 [c]13.5±1 [d]12.3±1	2.498 2.601 [c]2.666 [d]2.424	[c]11.1±0.2	[c]2.708
W	25.44±0.23	4.39±0.04	23.5±0.2 23.9±1 [c]24.2±1	4.046 4.119 [c]4.178	[c]23.8±0.2	[c]4.110
Re	-0.94±0.07	-0.42±0.03	3.9±0.2	1.73	----------	--------
Oy (^{235}U 93.2%; ^{238}U 6.8%)	126.022±1.25	+29.265±0.31	131.8±1 [c]132.1±1 [b]137.9±0.2	30.607 [c]30.676 [b]32.023	134.5±0.2 [c]134.4±0.2	31.224 [c]31.216
^{238}U	30.1±0.28	5.37±0.05	29.2±0.2	5.199	----------	--------

[a]Average of calculations with 500 and 600 percent dense samples.

[b]Exact central configuration in center of core.

[c]Sample cross sections averaged over reflector spectrum.

[d]Molybdenum density in radial reflector reduced to 0.95.

TABLE II. - COMPARISON OF CALCULATED AND MEASURED INTEGRAL

SAMPLE WORTHS AT SEVEN CENTRAL CORE LOCATIONS

[1.3-cm-diam by 37.5-cm-long samples.]

Material, m	Measured		Calculated			
			Four group		13 group	
	Worth, ¢	Specific worth, m¢/g	Worth, ¢ (a)	Specific worth, m¢/g	Worth, ¢ (a)	Specific worth, m¢/g
Li	-6.23±0.012	-33.07±0.061	-5.8	-30.8	-6.9 [b]-7.6	-36.5 [b]-40.4
^{6}Li(94.72%) ^{7}Li(5.20%)	-128.28±1.32	-871.86±9.51	-133.7	-908.7	-137.0	-925.5
^{7}Li(99.993%) ^{6}Li(0.007%)	6.18±0.07	36.65±0.41	6.3 [c]5.4	37.2 [c]31.9	5.7 [d]4.8	33.8 [d]28.6
$^{7}Li_3N$(95.62%) $^{7}Li_2O$(1.82%) $^{7}LiOH$(2.56%)	5.49±0.07	19.694±0.26	5.2	18.5	-------	--------
Be	44.80±0.41	68.71±0.63	19.3	29.38	-------	--------
BeO	37.90±0.34	37.11±0.33	23.4	22.84	-------	--------
^{10}B(92.01%) ^{11}B(7.99%) C(2.46%) O(0.95%) H_2O(0.05%)	-272.041±2.76	-717.12±8.49	-241.3	-636.18	-244.9 [e]-245.1	-645.57 [c]-646.10
C	18.69±0.15	30.94±0.25	16.7	27.65	17.9	29.52
Nb-1%Zr	-1.605±0.08	-0.565±0.03	-2.1	-0.741	-------	--------
Mo	4.73±0.07	1.31±0.02	-3.9	-1.07	-2.2	-0.602
Hf	-25.92±0.30	-5.80±0.07	-22.7	-4.916	-20.2	-4.386
Ta	-44.94±0.49	-7.65±0.08	-55.4	-9.359	-54.0	-9.114
W	-8.99±0.14	-1.33±0.02	-20.5	-3.036	-17.9	-2.649
Re	-34.37±0.39	-13.17±0.15	-26.9	-10.26	-------	--------
Oy (^{235}U 93.2%; ^{238}U 6.8%)	338.234±3.85 [f]383.44	77.432±0.82 [f]76.48	394.6 -----	78.54 -------	392.2 -------	78.068 --------
^{238}U(99.78%) ^{235}U(0.22%)	30.348±0.27	4.631±0.04	17.0	2.586	-------	--------

[a]Precision, ±0.2¢.

[b]Calculations with 500 percent dense samples.

[c]Average of calculations with 500 and 600 percent dense samples.

[d]Calculations with 600 percent dense samples.

[e]Mesh points in sample regions tripled.

[f]All drums full in.

TABLE III. - COMPARISON OF CALCULATED AND MEASURED

INTEGRAL SMALL SAMPLE WORTHS IN CENTER OF CORE

[1.35-cm-diam by 5.08-cm-long, thin-wall samples.]

Material, m	Measured		Calculated four group	
	Worth, ¢ (a)	Specific worth, m¢/g	Worth, ¢	Specific worth, m¢/g
^{6}Li	[b]-0.165	[b]-639±27	-0.357	-1384
^{7}Li	-.012	-41±24	.00866	29.8
^{10}B(92.01%) ^{11}B(7.99%)	-.946	-1159±8.6	-.890	-1090.6
Hf	-.093	-14.2±1.1	-.0628	-9.56
Ta	-.148	-14.9±0.7	-.143	-14.4
W	-.066	-7.2±0.8	-.0621	-6.74
Re	-.156	-19.6±0.9	-.141	-17.71
Oy ^{235}U 93.2%; (^{238}U 6.8%)	.517	86.1±1.2	.534	88.97
^{238}U(99.78%) ^{235}U(0.0022%)	.065	5.8±0.6	.0361	3.218

[a]Precision, ±0.007¢.

[b]Value may be in error due to leak in encapsulation.

The method of interpreting the spatial dependence of the reactivity of the large samples (that has been developed so as to combine the measured and calculated integral worth data to obtain spectrum-averaged cross-section correction factors) depends on the absence of significant resonance flux in the reactor spectrum. How well this requirement on the flux is fulfilled for the NCA composition 5 critical configuration neutron spectrum is shown in figure 2, which is the spectrum measured at the center of the core, and in figure 3 (from ref. 6), which is the spectrum measured at the core-reflector interface. These measurements were made using spherical shaped gas proportional counters and measuring the proton recoil pulse-height distribution. The neutron flux is negligible below 40 keV at both core locations.

The large depression in the flux near 250 keV, which is caused by the lithium resonances, tends to reduce the sensitivity of the cross-section correction method to cross-section errors occurring in this range. In table I calculations of the sample worth in the core spectrum are compared with sample worth in the molybdenum reflector spectrum, which is a degraded fission spectrum. It is seen that the difference in sample worths for the two spectra is small with the exception of lithium, molybdenum, and boron. This implies that the other materials investigated do not have especially important cross-section contributions near 250 keV.

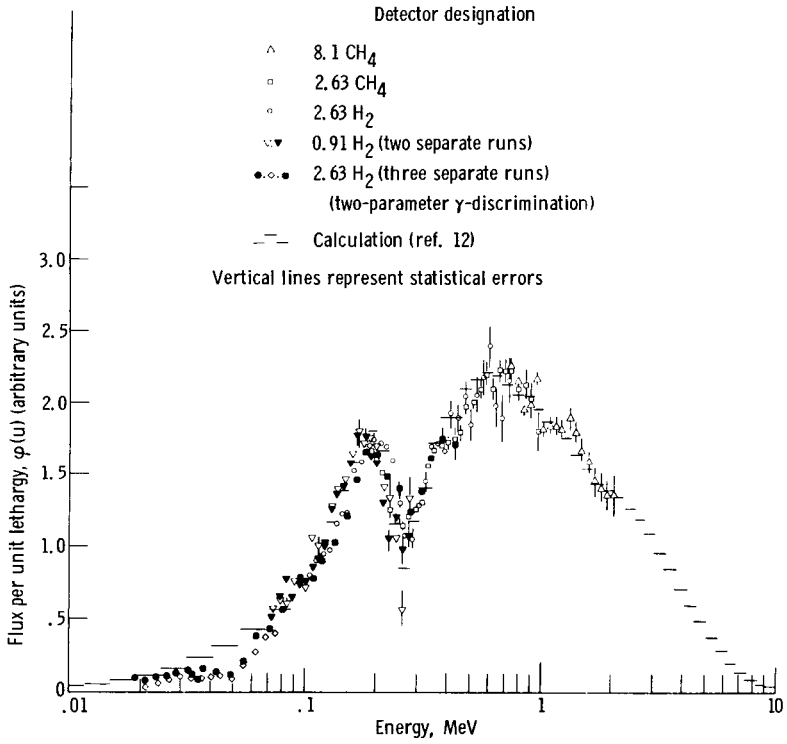

Figure 2. - Neutron spectrum in center of composition 5. (Numbers in detector designations denote pressure in atm.)

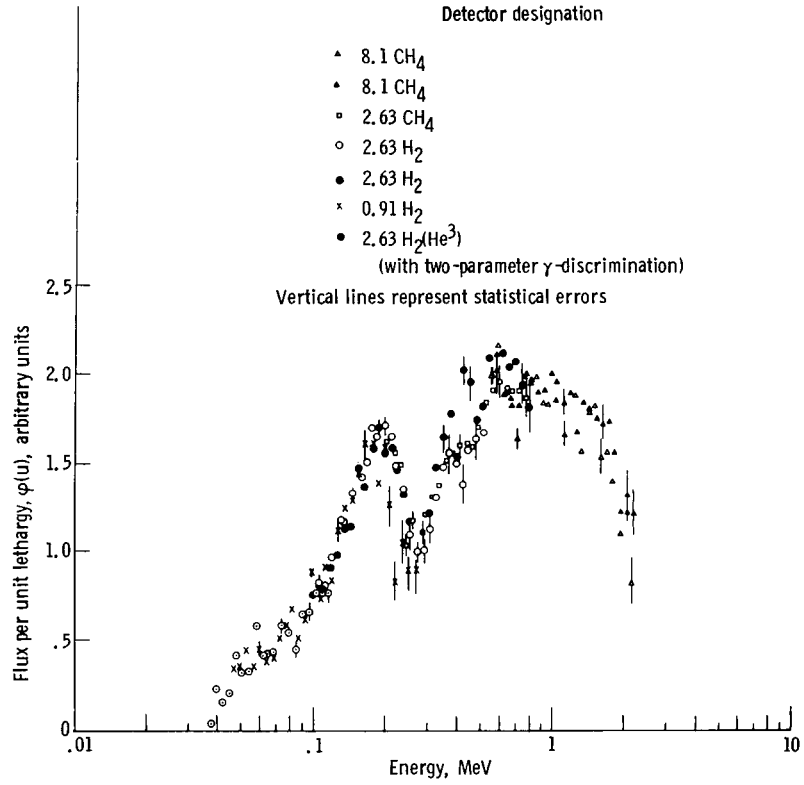

Figure 3. - Neutron spectrum at core-reflector interface. (Numbers in detector designations denote pressure in atm.)

TWO-DIMENSIONAL TRANSPORT ANALYSIS OF MATERIAL REPLACEMENT EXPERIMENTS

Large Samples at Peripheral Locations

Material samples in core. - The reactivity worth of the large samples at the edge of the core was calculated by the method of discrete ordinates as the difference of two eigenvalues for the reactor configuration in an xy geometrical representation. The GAM II code (ref. 3) 99-group cross sections were weighted over the computed assembly spectrum to obtain four- and 13-group cross-section sets above 0.414 electron volt (see table IV). The thermal neutron energy range was not included because of the negligible

TABLE IV. - ENERGY GROUP STRUCTURE

USED IN CALCULATIONS

Group number	Four-group set energy minimum[a], eV	Thirteen-group set energy minimum, eV
1	0.8209×10^{6}	3.6788×10^{6}
2	$.1832\times10^{6}$	2.2313
3	40.868×10^{3}	1.3533
4	$.414\times10^{0}$	.8209
5	----------	.6081
6	----------	.4979
7	----------	.3020
8	----------	.2237
9	----------	.1832
10	----------	.1111
11	----------	40.868×10^{3}
12	----------	15.034×10^{3}
13	----------	0.414×10^{0}

[a]Energy maximum, 14.9183×10^{6} eV.

thermal flux. Four- and 13-group region homogenized macroscopic P_0 cross sections obtained from the MACROS and MACRUP data handling programs were used in the transport theory TDSN (ref. 7) program for the four-group S_4 calculations and in the DOT (ref. 8) program for the 13-group S_4 calculations using the geometrical representation given in figure 4.

In this figure the midplane geometry of the critical assembly was accurately reproduced by the stepped core boundaries and the explicit representation of the fueled and absorber drum regions and the molybdenum reflector regions. The cylindrical samples

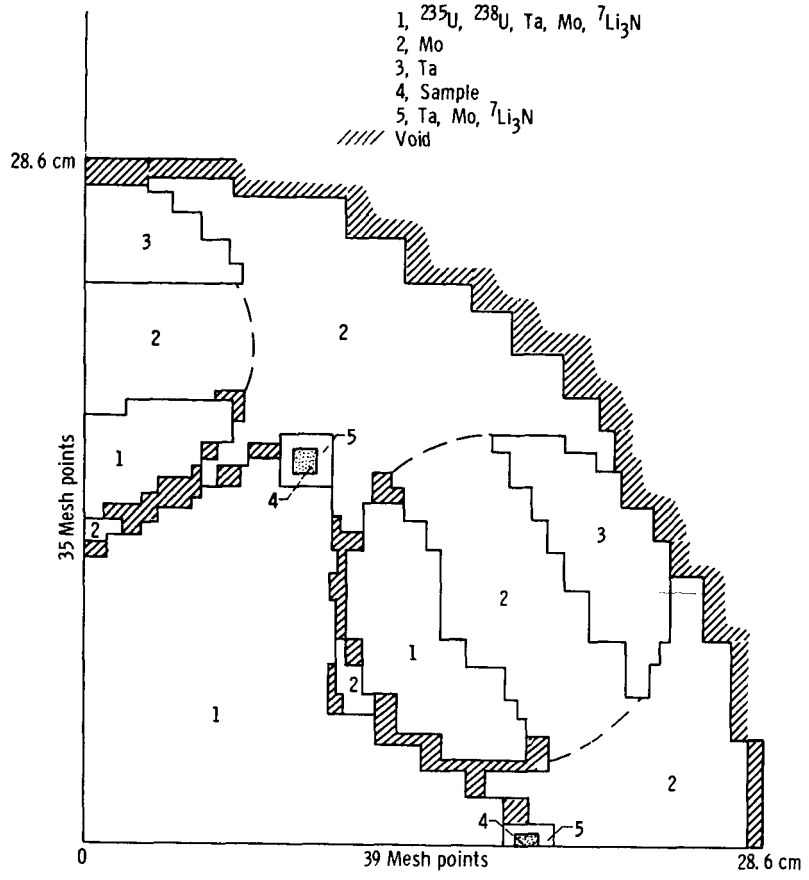

Figure 4. - XY model of critical experiment.

were represented by square regions of nearly equal area at the correct radial locations.

In the calculational geometry the core was uniformly loaded with fuel. In the experimental configurations the loading of the seven central fuel elements was adjusted as required to make the core nearly critical either with the positive-worth edge samples inserted or the negative-worth edge samples withdrawn so that the interchange of sample and void resulted in a declining flux-time profile as required by the inverse kinetics analysis program. Experimental and analytical investigation showed that this readjustment of the central fuel loading had a negligible effect on the measured sample worth and that the assumption of a uniform core loading in the analysis leads to a calculational error of less than ±3 percent in sample worth (see RESULTS section).

The transverse leakage was taken into account by the incorporation of an effective core height in the multigroup transport theory programs. The effective core heights were obtained from two-dimensional RZ four-group TDSN and 13-group DOT calculations in which all the geometrical details in the axial direction were explicitly represented.

The region around the reactivity sample locations (region 5 in fig. 4) contained the

lithium-7 nitride ($^7Li_3N$), the tantalum tubing, and the molybdenum sample cladding associated with the sample locations in a smeared fashion. Table I lists the materials measured.

Void reference samples in core. - The eigenvalue difference method gives the sample worth by subtracting the reactivity calculated with the voided sample in the core from the reactivity calculated with the material sample in the core. Because the voided samples created end effects (core-reflector interactions with sample location voided) and void leakage (streaming) components that could not be satisfactorily treated with two-dimensional transport theory, an additional experiment was performed in which the excess reactivity of the critical assembly with the sample locations voided was measured. The geometry and fuel loading were duplicated in two-dimensional xy 4-group TDSN and 13-group DOT transport calculations of the excess reactivity.

Present calculational procedures overestimate the absolute magnitude of the eigenvalue of the NCA critical configuration by several percent because of errors in the tabulated cross sections, the reduced order of the angular segmentation and the scattering expansion, and the coarse-group structure (ref. 9). This overprediction or bias in the absolute value of the reactivity was determined for a number of the NCA critical configurations and is shown as a function of uniform fuel loading in figures 5 and 6. Also shown on these plots is the excess reactivity calculated for the void sample experiment. The difference between the excess reactivity computed for the void sample experiment and the bias computed for a uniformly loaded core containing the same amount of fuel is 6.3±0.1 cents for both the four-group and 13-group analysis. This difference is attributed to end

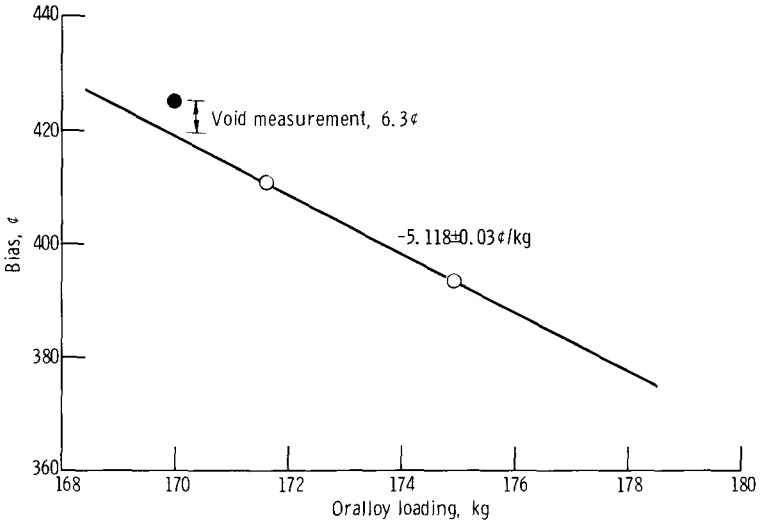

Figure 5. - Calculational bias as function of oralloy loading for XY calculations (four-group calculations). NASA heavy-metal-reflected, fast-spectrum critical assembly configurations. Error on calculated points, ±0.07 cent.

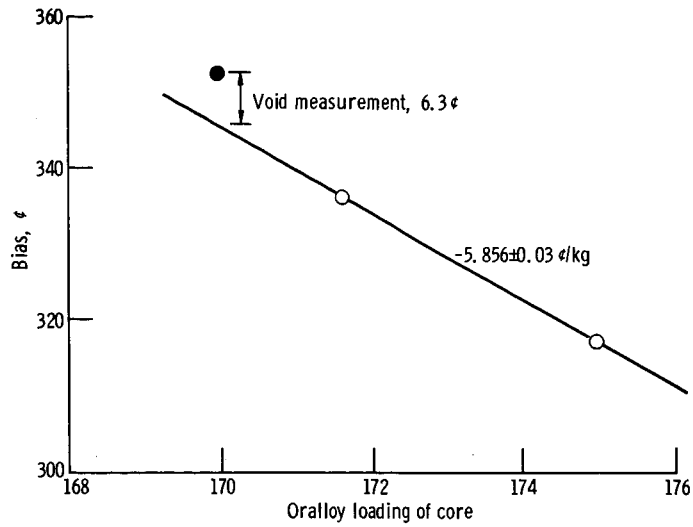

Figure 6. - Calculational bias as function of oralloy loading for XY calculations (13-group calculations). NASA heavy-metal-reflected, fast-spectrum critical assembly configurations. Error on calculated points, ±0.07 cent.

effects and void leakage components which are neglected in the two-dimensional analysis. The void sample calculations used for eigenvalue difference computations were corrected for this neglect by reducing the calculated eigenvalue by 6.3 cents.

For the oralloy samples an additional 22.0±0.1 and 25.2±0.1 cents was added to the eigenvalue difference for the four-group and 13-group calculations, respectively, to account for the shift in bias due to the increased oralloy loading associated with these samples, as stipulated in figures 5 and 6.

Transverse reactor leakage cross sections. - The transverse buckling-loss cross section (DB^2) is computed in TDSN and DOT for each material region using the relation:

$$DB^2 = \frac{\pi^2}{3\left(\Sigma_{TR}H + 2\gamma\right)^2}\Sigma_{TR}$$

where H is the effective core height obtained from two-dimensional RZ calculation, Σ_{TR} is the macroscopic transport cross section, and $\gamma = 0.7104$. This relation incorporates the competing effects of (1) a decrease in the buckling-loss cross section due to a decrease in the diffusion constant with increasing transport cross section, and (2) an increase in the buckling-loss cross section due to an increase in the buckling resulting from a decline in the extrapolation length with increasing transport cross section. Hence, the buckling-loss cross section attains a maximum at $\Sigma_{TR} = (2\gamma/H)$ ($\sim 0.025\ cm^{-1}$ for $H = 56.8$ cm) and approaches zero as Σ_{TR} approaches zero. This means that the

computed axial leakage probability for transparent sample regions does not approach the correct limit for small Σ_{TR}. Since the relation is correct for moderate values of Σ_{TR}, an investigation was conducted to determine the bounding value of the transport cross section above which anomalous behavior in the buckling-loss cross section would not be expected for the samples.

A series of calculations of the specific worth (m¢/g) of scattering materials having intrinsically small absorption cross sections and positioned in the six edge sample locations were performed. The results are shown in figures 7 and 8, in which the specific worth is plotted against density of the material. The decrease in calculated edge worths for lithium-7 (^{7}Li) and carbon (C) at small values of the transport cross section (density) is the result of the anomaly in the calculated transverse leakage cross section. The slight decrease seen for large values of the transport cross section is expected because of saturation effects. On the other hand, the edge worth calculations for the absorbers ^{6}Li and boron-10 (^{10}B) shown in figures 9 and 10 do not show the anomalous behavior at small values of the transport cross section, indicating the mitigating effect of strong absorption. It is concluded that the buckling-loss cross sections are correctly computed for predominantly scattering regions if the transport cross sections are greater than 0.15 reciprocal centimeter.

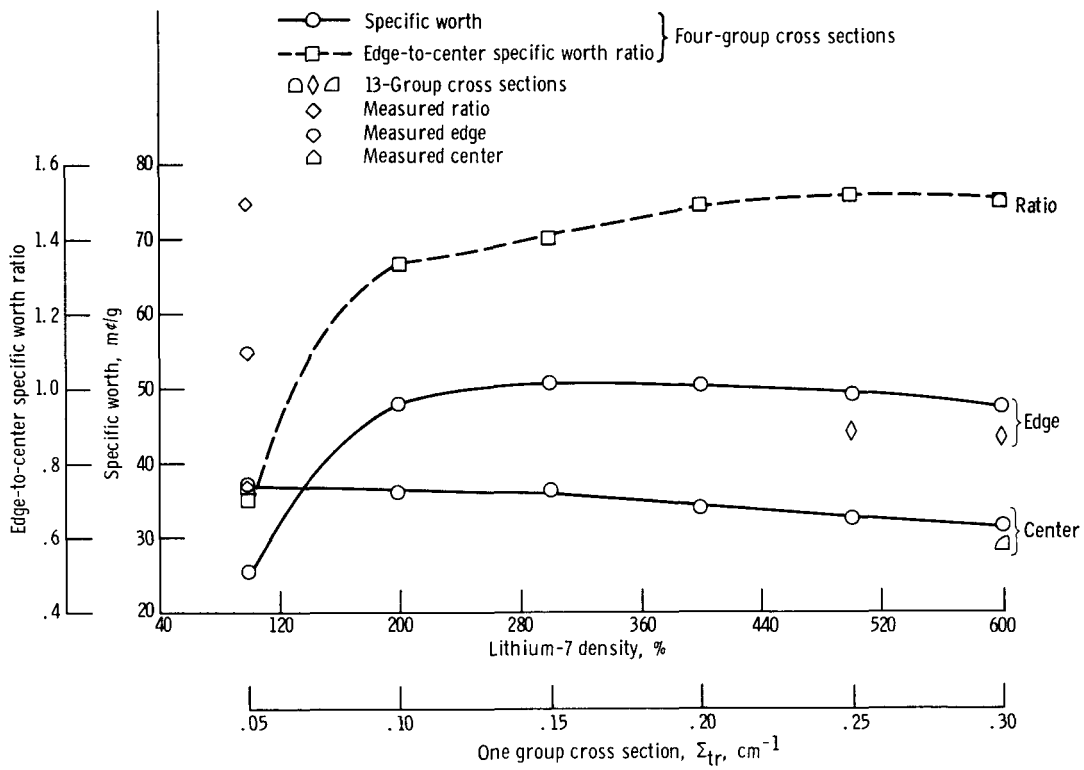

Figure 7. - Measured and calculated center and edge specific integral worth and edge-to-center specific integral worth ratio as functions of lithium-7 sample density and cross section.

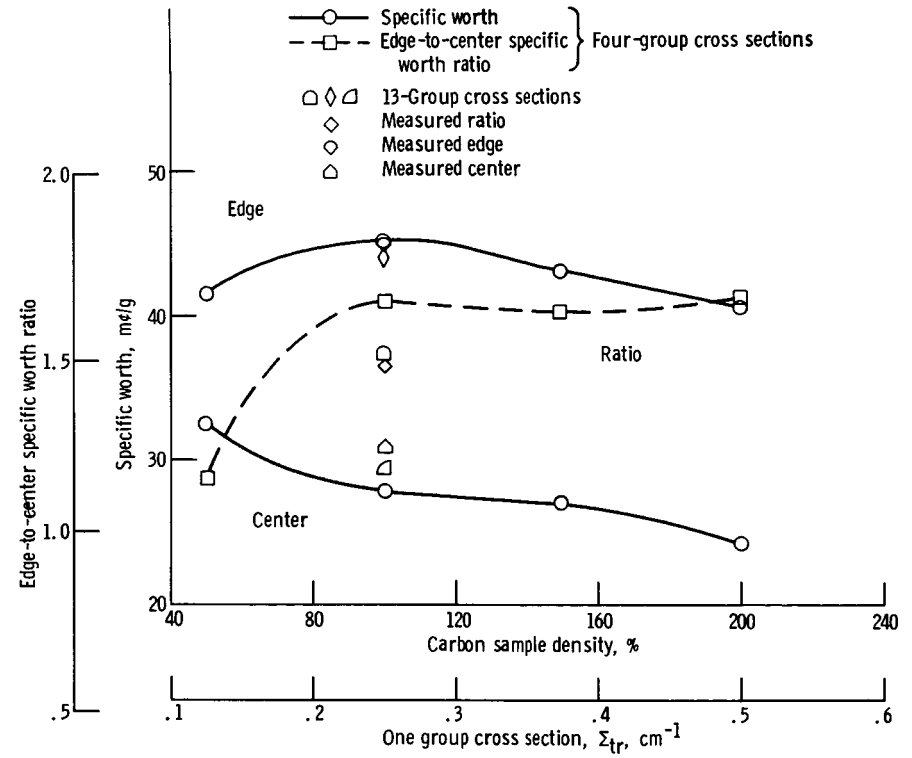

Figure 8. - Measured and calculated center and edge specific integral worth and edge-to-center specific integral worth ratio as functions of carbon sample density and cross section.

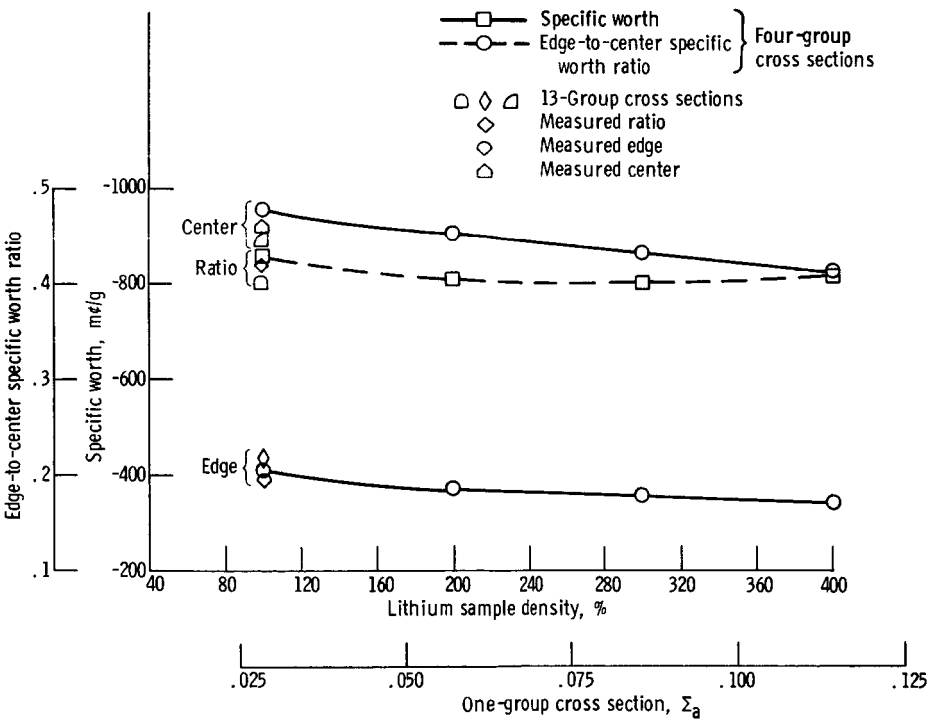

Figure 9. - Measured and calculated center and edge specific integral worth and edge-to-center specific integral worth ratios as functions of lithium sample density and cross section. (Corrected for scattering.)

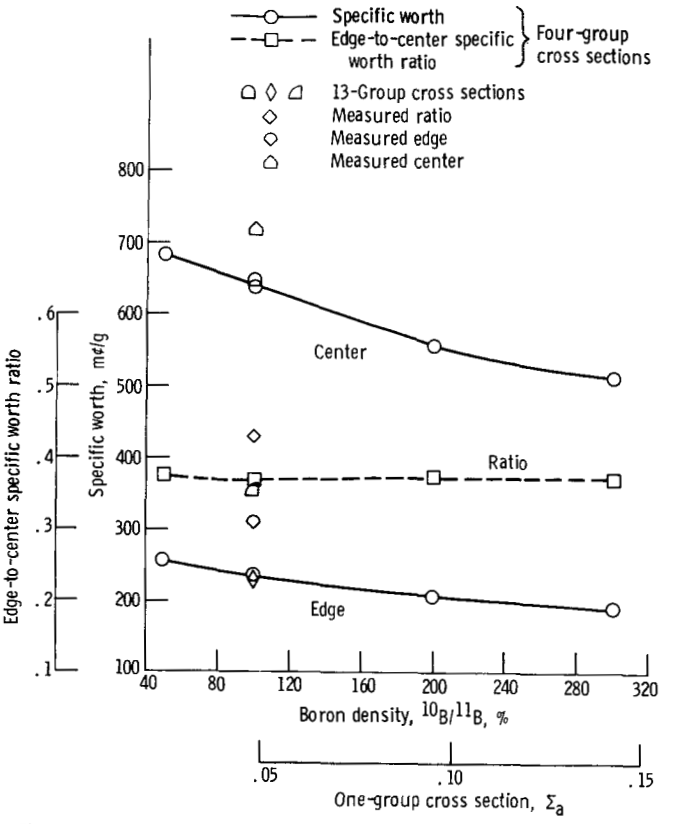

Figure 10. - Measured and calculated center and edge specific integral worth and edge-to-center specific integral worth ratio as functions boron-10 - boron-11 sample density. (Corrected for scattering.)

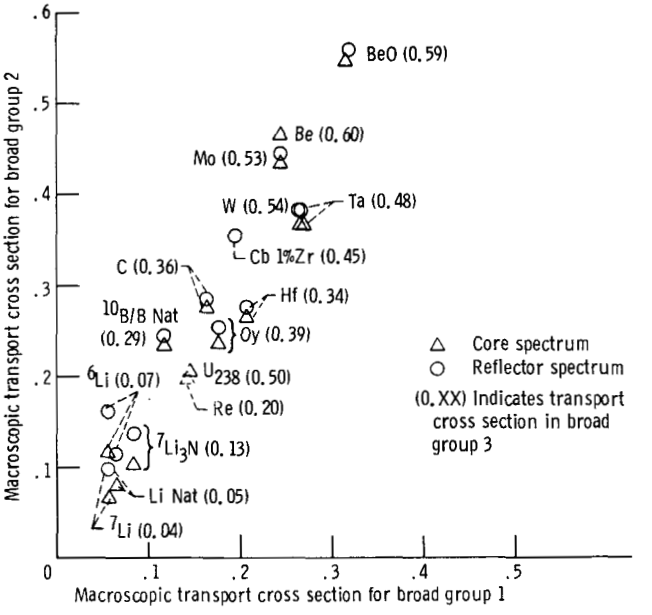

Figure 11. - Sample transport cross section for groups 1 to 3 of four-group set averaged over core and reflector spectrum.

The magnitude of the transport cross section for the top three groups, which contain 97.4 percent of the flux in the four-group TDSN calculation, are plotted in figure 11 for all sample materials. With the exception of the Li samples, all sample transport cross sections are greater than 0.15 reciprocal centimeter and, hence, are not subject to the buckling loss cross section anomaly. The integral specific worths at the edge of the core for natural Li, ^{7}Li, and $^{7}Li_3N$ were calculated using sample densities of 500 and 600 percent of the actual value to eliminate the buckling-loss cross section anomaly.

Large Samples in Central Locations

Eigenvalue difference methods using a cylindrical RZ geometrical representation in four-group TDSN and 13-group DOT S_4 transport theory calculations were used to obtain the sample worths in the seven central core locations. Ninety-nine group GAM II cross sections weighted over the computed assembly spectrum and region homogenized by the MACROS and MACRUP data handling programs provided four and 13 broad-group P_0 input cross sections for the transport programs. Calculations below 0.414 electron volt were omitted because of the negligible number of neutrons in this range. The energy breakdown is given in table IV.

Figure 12 depicts the RZ representation used for these calculations. The central cylindrical sample is explicitly treated while the surrounding six cylindrical samples in the first ring are homogenized with the $^{7}Li_3N$, tantalum (Ta) cladding, molybdenum (Mo) tubing, and void within the annulus defined by the samples. The axial reflector adjacent to the sample region contains the additional Mo and Ta tubing associated with the sample changer in a smeared fashion. The RZ calculational geometry incorporated the voids into the calculation. This method of incorporating the voids in the calculations accounts for the major void effects as demonstrated later by the good agreement with experiment obtained for the sample worths of well known materials such as carbon. Thus corrections for discrete sample void and end effects are not required. Table II specifies the material samples measured.

The oralloy loading of the core in the calculations was uniform. The control drums were taken to be turned to the fuel full-in position. It was experimentally verified that difference in the central sample worth measured with the control drums turned full-in and with the control drums equally banked as in the measurements was less than 1.3 percent of the sample worth. These comparisons are shown in table II.

The overprediction or bias in the eigenvalue for the uniformly fueled cores as a function of fuel loading discussed earlier was recalculated in four and 13 groups in the RZ geometry. The results were similar to those shown in figures 5 and 6. As before, the calculated worths of the oralloy samples were increased by 43.4 and 38.9 cents for the

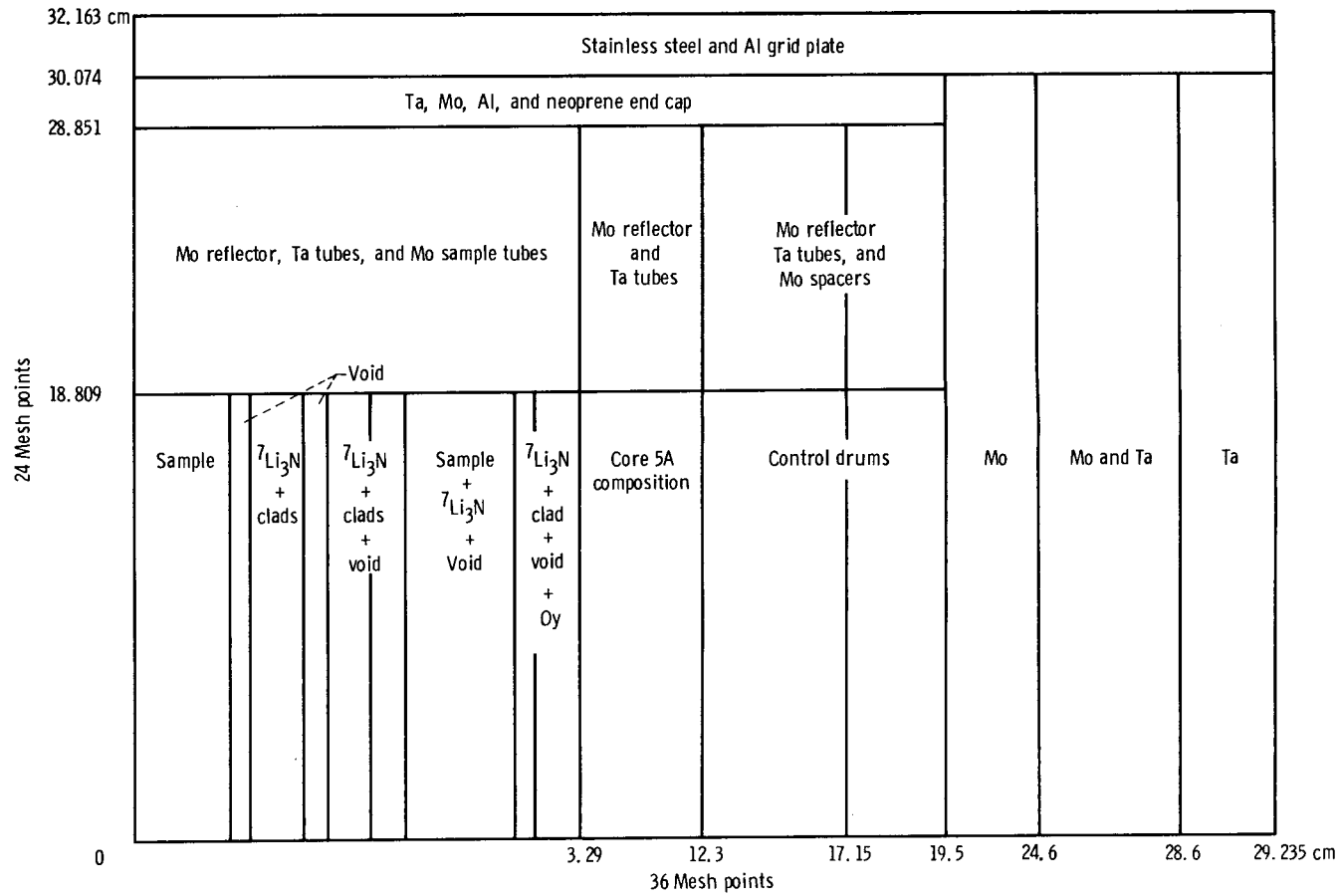

Figure 12. - RZ model of critical experiment for large central sample calculations. (Note nonlinear scale.)

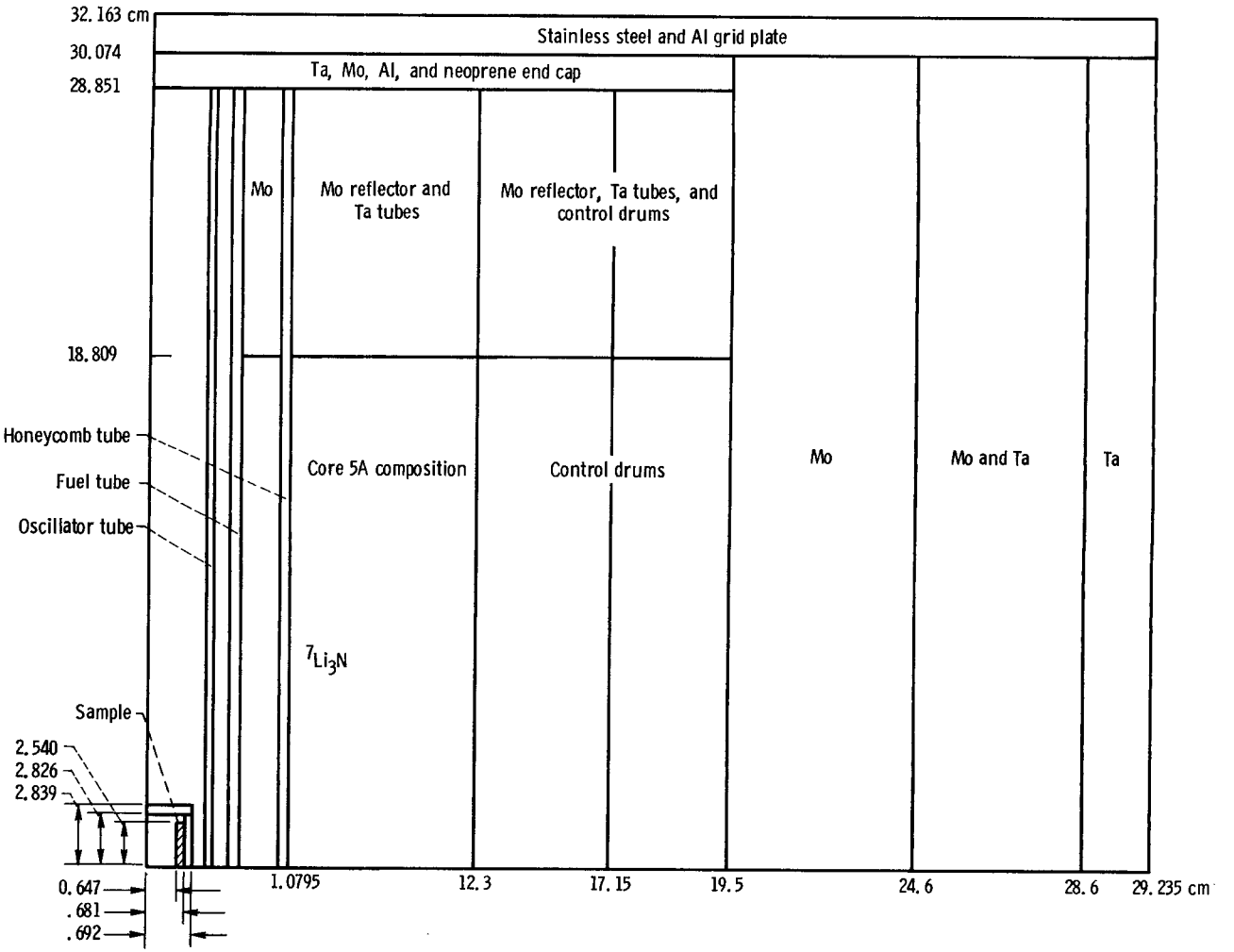

Figure 13. - RZ model of critical experiment for small central sample calculations. (Nonlinear scale.)

four and 13 groups, respectively, to account for the shift in calculational bias due to the overall increase in core loading with the oralloy samples inserted.

Dilute Samples in Center of Core

The calculations of the dilute sample worths were made using the PERTRAN (ref. 10) perturbation theory analysis program but were limited to transport corrected diffusion approximations because of computer memory limitations connected with the TDSN transport theory program. TDSN supplied volumes, radial and axial mesh boundaries, real and adjoint fluxes, and real and adjoint weighted production values for incorporation into the PERTRAN computations.

Figure 13 exhibits the RZ analytical configuration, in which the dilute samples are represented as 0.647 centimeter-inside-radius, 0.034-centimeter-thick, 5.08-centimeter-long cylinders centered in the core. The samples are specified in table III. Explicit representation of the tantalum sample oscillator tube, tantalum fuel, and honeycomb tubes and the $^{7}Li_{3}N$ extensions through the axial reflector was made. The remainder of the assembly was smeared into core, drum, and reflector regions.

CROSS SECTION CORRECTION

Basis of Method

Engle, Hansen, and Paxton in their compilation of integral worth data of various materials measured in the Topsy, Godiva, and Jezebel critical assemblies (ref. 2) found that with the major exceptions of hydrogenous and fuel materials, that the integral worths for material x could be separated into the absorption and scattering components σ_a and σ_{tr} and that the integral worths were closely given by

$$\Delta k_0(r,x) = -\sigma_a(x)f_0(r) + \sigma_{tr}(x)f_1(r)$$

where $f_0(r)$ and $f_1(r)$ are functions of radius alone as is expected from one group diffusion theory. This one broad group approach was considered applicable to the present NCA integral worth measurements and calculations because of the absence of significant flux below 40 keV in this assembly (see figs. 2 and 3) and because of the remarkably flat adjoint flux above 40 keV at both the center and edge sample locations (figs. 14 and 15). Also implicit in this approach was the assumption that the inelastic scattering of the sample does not significantly alter the asymptotic flux spectrum.

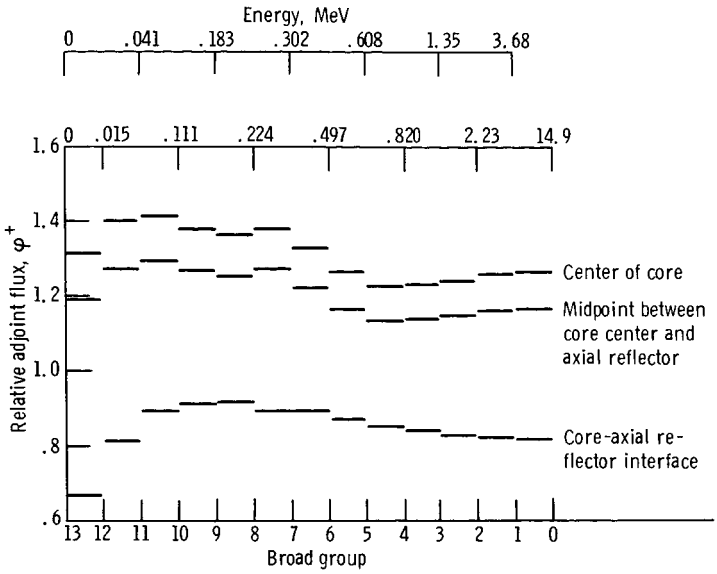

Figure 14. - Thirteen group, PoS_4, 2D RZ transport theory calculations of unperturbed adjoint flux in central sample location.

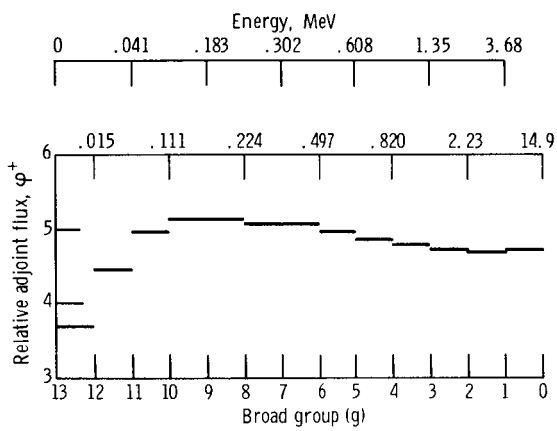

Figure 15. - Thirteen group PoS_4 2D XY transport theory calculations of unperturbed adjoint flux at edge sample location (core midplane).

In the present analysis, both the measured and calculated integral worths at the center and the edge of the core are separated into integral absorption and scattering components for each material. To perform the separation, coefficients analogous to $f_0(r)$ and $f_1(r)$ were obtained from the measured integral worths of the predominant scatterers C and ^7Li and the predominant absorbers ^6Li and $^{10}B/^{11}B$ as corrected to remove scattering effects. Comparison of the calculated and measured scattering components then yielded a fast-spectrum-averaged absorption and scattering correction factor for each material. The ratio $^{10}B/^{11}B$ refers to the 92.01 percent ^{10}B, 7.99 percent boron

composition of the samples.

These correction factors were then incorporated into the GAM II cross section set used in the analysis with the result that the calculated integral worths are brought into close agreement with measurement as required. Core design calculations were then repeated using the improved cross-section set, and it was found that known calculational biases attributed to cross-section errors were substantially reduced. In practice correction factors obtained by applying this method to other cross section sets can be used to point out significant inconsistencies in magnitude in the cross section tabulations used to generate the macroscopic cross section set.

Partition of Integral Worth into Absorption and Scattering Components

Engle, Hansen, and Paxton base their separability arguments on spherical cores only. The NCA core in which the full-core-length material replacement worth measurements were made is two-dimensional and cylindrical, and the axial worth distribution is different at the central sample locations and at the core-reflector interface sample locations. To include the radial dependence of the axial worth distribution, the integral worth for the sample material m was partitioned as follows:

$$W(r,m) = \int_{-L/2}^{L/2} C_A(r,z,m)dz + \int_{-L/2}^{L/2} C_s(r,z,m)dz \qquad (1)$$

where $W(r,m)$ is the full-length integral reactivity worth in millicents per gram for the material m at the radial position r and $\int_{-L/2}^{L/2} C_A(r,z,m)dz$ and $\int_{-L/2}^{L/2} C_s(r,z,m)dz$ are the absorptive and scattering components, respectively, for the material m at r and z integrated over the length L of the sample.

The validity of the separability assumption was checked by comparing the ratio of the specific integral worth measured at the edge of the core $r = R$ with the specific integral worth measured at the center of the core $r = 0$, for two "pure" scatterers (absorption component equals zero) having very different cross section shapes, using equation (1).

$$\left.\begin{aligned} \frac{W(R,m)}{W(0,m)} = \frac{\int_{-L/2}^{L/2} C_s(R,z,m)dz}{\int_{-L/2}^{L/2} C_s(0,z,m)dz} &= 1.46 \text{ for carbon} \\ &= 1.49 \text{ for } {}^7\text{Li} \end{aligned}\right\} \qquad (2)$$

The ratios of the edge-to-center integral worth for two predominant absorbers analytically corrected for scattering (scattering component equals zero) were also compared:

$$\left.\begin{aligned}\frac{W(R,m)}{W(0,m)} = \frac{\int_{-L/2}^{L/2} C_A(R,z,m)dz}{\int_{-L/2}^{L/2} C_A(0,z,m)dz} &= 0.422 \quad \text{for } {}^{6}\text{Li} \\ &= 0.427 \quad \text{for } {}^{10}\text{B}/{}^{11}\text{B}\end{aligned}\right\} \tag{3}$$

These ratios agree within 2 percent for materials having very different cross section shapes, thus confirming the separability assumption.

Calculated edge-to-center ratios over a useful range of cross section values are compared with measurement in figures 7 to 10. The agreement between experiment and calculation for these ratios, which were shown to be essentially independent of cross section, should be an indication of the accuracy of the geometrical representation of the core in the calculation and the validity of the corrections used to account for the end effects and the void leakage effects. However, there is some scatter in the agreement between the four- and 13-group results. The calculated ratio for boron is in poor agreement with measurement in both the four- and 13-group treatment, so that a value of the average deviation would not be meaningful. Since carbon has a well known cross-section structure, the best indication of the accuracy of the analytical geometry and technique is the 1.8-percent deivation obtained between the 13-group calculated edge-to-center ratio and the measurement ratio for carbon (fig. 8).

Figures 7 to 10 show that the edge-to-center worth ratios are reasonably constant over the range of cross-section magnitude and shape encountered in the material samples. Hence, it is concluded that for this critical assembly composition the edge-to-center ratio of specific integral worth for an absorber is constant, independent of the shape or magnitude of the cross section of the absorber, and that the ratio of the edge-to-center specific integral worth for a scatterer is constant, independent of the shape or magnitude of the scattering cross section. Thus equation (1) is valid for all nonhydrogenous and nonfissile materials in the NCA 5 spectrum. Therefore, equations for material m can be written for the central and edge sample integral worth using the average measured coefficients given in equations (2) and (3).

$$W_M(0,m) = \int_{-L/2}^{L/2} C_A(0,z,m)dz + \int_{-L/2}^{L/2} C_S(0,z,m)dz \tag{4}$$

$$W_M(R,m) = 0.425 \int_{-L/2}^{L/2} C_A(0,z,m)dz + 1.48 \int_{-L/2}^{L/2} C_s(0,z,m)dz \quad (5)$$

The measured specific full-length integral worths at the edge and the center of the core can then be substituted for $W_M(0,m)$ and $W_M(R,m)$ and equations (4) and (5) solved for $\int_{-L/2}^{L/2} C_A(0,z,m)dz$ and $\int_{-L/2}^{L/2} C_s(0,z,m)dz$ the full-length absorptive and scattering components for material m at the center of the core. In this manner, the measured integral worth is partitioned into components.

Computation of Cross-Section Correction Factors

The calculated integral specific worths for each material m can also be partitioned in an analogous fashion:

$$W_c(0,m) = \frac{1}{A_m} \int_{-L/2}^{L/2} C_A(0,z,m)dz + \frac{1}{S_m} \int_{-L/2}^{L/2} C_s(0,z,m)dz \quad (6)$$

$$W_c(R,m) = \frac{0.425}{A_m} \int_{-L/2}^{L/2} C_A(0,z,m)dz + \frac{1.48}{S_m} \int_{-L/2}^{L/2} C_s(0,z,m)dz \quad (7)$$

where $W_c(0,m)$ and $W_c(R,m)$ are the calculated integral specific worths at the center and at the edge of the core, respectively, and $\int_{-L/2}^{L/2} C_A(0,z,m)dz$ and $\int_{-L/2}^{L/2} C_s(0,z,m)dz$ are the measured material absorptive and scattering components obtained previously. Equations (6) and (7) are solved for A_m and S_m, the absorptive and scattering spectrum averaged cross-section correction factors for material m.

The role of A_m in equations (6) and (7) becomes apparent by considering the case of a pure absorber, for which case

$$W_c(0,m) = \frac{1}{A_m} \int_{-L/2}^{L/2} C_A(0,z,m)dz \quad (8)$$

$$W_c(R,m) = 0.425 \frac{1}{A_m} \int_{-L/2}^{L/2} C_A(0,z,m)dz \tag{9}$$

However, for a pure absorber equations (4) and (5) become

$$W_M(0,m) = \int_{-L/2}^{L/2} C_A(0,z,m)dz$$

$$W_M(R,m) = 0.425 \int_{-L/2}^{L/2} C_A(0,z,m)dz$$

and equations (8) and (9) can be written as

$$W_c(0,m) = \frac{1}{A_M} W_M(0,m) \rightarrow A_m = \frac{W_M(0,m)}{W_c(0,m)}$$

$$W_c(R,m) = \frac{1}{A_m} W_M(R,m) \rightarrow A_m = \frac{W_M(R,m)}{W_c(R,m)}$$

where A_m is the factor by which the measurements differ from the calculations at both the center and the edge of the core. Therefore, multiplication of the analytical absorption cross section by A_m will bring agreement with measurement for the integral worths. This same argument can be applied to a pure scatterer and by induction to the case of a combined absorbing and scattering material.

Spectrum-Averaged Correction Factors to Sample Material Cross Sections

Equations (4) and (5) were solved for each sample material to obtain $\int_{-L/2}^{L/2} C_A(0,z,m)dz$ and $\int_{-L/2}^{L/2} C_s(0,z,m)dz$, the material absorptive and scattering components for each sample material, and then equations (6) and (7) were solved for A_m and S_m, the spectrum-averaged cross-section correction factors for each material. Insight into the ability of the formulation given in equations (4) and (5) to partition the measured central and edge integral worths into the material absorptive and scattering components is given in table V. Here, material absorptive components for a number of com-

TABLE V. - COMPARISON OF MEASURED SMALL SAMPLE WORTHS AND LARGE SAMPLE ABSORPTION COMPONENTS

Material, m	Small sample integral worth, m¢/g	Large sample absorption component, $\int_{L/2}^{L/2} C_A(0,z,m)dz$
Hf	-14.2	-10.9
Ta	-14.9	-12.6
W	-7.2	-6.03
Re	-19.6	-18.1

bined and scattering materials are compared with the central, small-sample specific integral worth, which essentially is a measure of the absorption in the sample. The comparison shows that material absorptive component is on the average 0.84 of the measured small sample worth in each case. The maximum deviation from the average is ≤9 percent. The material absorptive component is expected to be less negative than the small sample worth because the material absorptive component is derived from full-length measurements, which are the average of low-worth regions near the top and bottom of the core and high-worth regions at the center of the core. The point is that the computed material absorptive components are in good agreement with the measured worths for the small, highly absorptive samples, when these are normalized to reflect the full-length characteristic of the large samples. This is further evidence of the validity of partition into absorption and scattering components using equations (4) and (5).

Application of Correction Factors to Cross-Section Set

The GAM II cross-section set was adjusted to incorporate the correction factors as follows:

Transport cross section -

$$\sigma_{tr}^{*} = S_m(\sigma_{tr} - \sigma_a) + A_m\sigma_a \tag{10}$$

Absorption cross section -

$$\sigma_a^{*} = A_m\sigma_a \tag{11}$$

Total transfer matrix -

$$\sigma^{*}_{g\to g'} = S_m \sigma_{g\to g'} \tag{12}$$

The starred values are the corrected cross sections and the unlabeled values are the four- and 13-group cross sections obtained from GAM II.

The corrections were applied uniformly to all of the groups. Hence, any inaccuracies in the cross-section shape and in the inelastic scattering model are not treated by this procedure.

RESULTS

Comparison Between GAM II Calculations and Measurement

Comparison of integral sample worths. - Tables I and II compare the measured and calculated integral sample worths at the center seven sample locations and at the six core edge locations. Table III compares the central small sample worths. The tables list the material calculated together with the impurities included in the calculations. The sample worths were calculated using 99-group cross sections weighted over the core spectrum unless noted. At the six edge locations most of the results were obtained using 99-group cross sections weighted over the molybdenum reflector spectrum, since this spectrum probably is more representative of the physical situation. However, the use of reflector spectrum weighting made little difference in the value of the calculated worth; the largest difference is 14 percent occurring for ^{6}Li. In general though, the molybdenum spectrum calculations are in slightly better agreement with measurement.

That there is so little difference in integral worth when the molybdenum spectrum (which is essentially a degraded fission spectrum) is used in place of the very different core spectrum (fig. 2) shows that the integral worth in the fast spectrum neutron range is not very sensitive to the shape of the interaction density $\Sigma(E)\varphi(E)$ and, therefore, not very sensitive to the cross-section shape. The reason for the insensitivity to cross-section shape is that the adjoint flux is remarkably constant over the spectrum range of importance as shown in figures 14 and 15. These analytical conclusions are in agreement with the earlier experimental finding that the ratio of the edge-to-center specific worth is constant for all predominant absorbers and for all predominant scatterers independent of cross-section shape or magnitude.

In order to demonstrate that self-shielding effects are negligible over the fast-spectrum range under consideration, the $^{10}B/^{11}B$ calculations at the center of the core were repeated for the large samples with number of mesh points in each region tripled.

The mesh spacing for the center sample was decreased from 0.327 to 0.109 centimeter, while the mesh spacing for the six samples in the first ring around the center was decreased from 0.654 to 0.218 centimeter. The difference in integral worth was less than 0.1 percent as is seen in table II.

Table I contains entries for ^{6}Li and Oy for which the calculations were made using the exact experimental core loading in the central seven fuel elements in place of the uniform core loading assumed for the standard calculations. The calculational error associated with the standard calculation is less than ±3 percent.

A comparison of calculated and measured small sample integral worths is given in table III. It is believed that the ^{6}Li measurement is in error since subsequent inspection of the sample revealed chemical activity with the atmosphere probably caused by a leak in the encapsulation. The ^{7}Li value also seems doubtful because it is inconceivable that a predominant scatterer would yield a negative integral worth value at the center of the core.

Deviation in percent between calculation and experiment. - The most reliable calculated integral worths for each material have been abstracted from tables I to III and are

TABLE VI. - DIFFERENCE IN PERCENT BETWEEN CALCULATED AND EXPERIMENTAL INTEGRAL WORTHS

[Positive values indicate a more positive calculated integral worth.]

Material, m	Center large samples		Center small samples	Edge large samples	
	Four group	13 group	Four group	Four group	13 group
Li	6.8	-10	-------	-24	-27
^{6}Li	-4.3	-6.2	[a]-116	[b]4.6	------
				-6.2	-.26
^{7}Li	1.5	-7.9	172	-12	-20
$^{7}Li_3N$	-6.1	------	-------	-18	------
Be	-57	------	-------	-5.8	------
BeO	-38	------	-------	4.5	------
$^{10}B/^{11}B$	11	10	5.9	28	30
C	-11	-4.5	-------	.38	-2.9
Nb-1%Zr	-31	------	-------	6.0	------
Mo	-182	-146	-------	4.7	2.3
Hf	15	24	33	40	43
Ta	-22	-19	3.4	33	35
W	-128	-99	6.8	-4.2	-6.4
Re	22	------	9.6	511	------
Oy	1.4	.82	3.3	4.8	6.6
^{238}U	-44	------	-44	-3.2	------

[a]Value may be in error because of leak in encapsulation.

[b]Exact central configuration.

compared with the measured value on a percent basis in table VI. In general the best agreement is obtained for principally absorbing materials in the center of the core, while at the edge of the core somewhat better agreement is found for the scattering materials. The 13-group calculations do not provide better agreement than the four-group calculations, again demonstrating the insensitivity of the integral worths to cross section shape. With the exception of ^{6}Li and ^{7}Li, which are believed to be erroneous, the small-sample worths agree somewhat better with experiment than the large central samples. This is possibly due to the fact that the absorption cross section is the factor being tested in this comparison of small-sample worths, so that scattering effects are insignificant in the case of the small-sample measurements. It is thus evident that comparison of small, central sample measurements with calculations are not sufficient to test the consistency of cross sections and that much more stringent tests with large samples at the core extremes are required.

Spectrum-Averaged Correction Factors to Sample Material Cross Sections

The spectrum-averaged cross-section correction factors are given in table VII for four-group and 13-group analysis. There is good agreement between the four- and 13-group values (1) of A_m, for the materials in which absorption is dominant, (2) of S_m, for the materials in which scattering is dominant, and (3) of both A_m and A_s, when the material has a mixture of absorption and scattering. In some cases the computed absorptive correction factors were negative (footnote (a)). These occurred for materials in which the absorption cross sections were insignificant such that small errors in the scattering formulation could force the compensating absorptive correction factor to go negative because it was operating on a very small cross section. The footnoted values correspond to the materials that are of special interest to the advanced reactor program and for which the correction factors were somewhat large. For these materials, the initially determined correction factors were applied to the cross section set; the sample worth calculations were repeated; and new correction factors were recomputed. This procedure was then repeated until successively computed correction factors agreed within a few percent. For these cases the correction factors changed less than 7 percent as a result of this iteration. Of course the recalculated edge and center worths were brought into very close agreement with their measured counterparts by this procedure.

TABLE VII. - SPECTRUM AVERAGED CORRECTION FACTORS TO

ABSORPTIVE AND SCATTERING CROSS SECTION

Material, m	Four group		13 group	
	Absorptive correction factor, A_m	Scattering correction factor, S_m	Absorptive correction factor, A_m	Scattering correction factor, S_m
Li	1.15	1.22	1.03	1.17
^{6}Li	.965	1.06	.926	.739
^{7}Li	.584	1.13	(a)	1.27
$^{7}Li_3N$	1.99	1.31	-----	-----
Be	(a)	.719	-----	-----
BeO	(a)	.780	-----	-----
$^{10}B/^{11}B$	1.06	.563	1.03	.502
^{10}B	[b]1.13	[b].290	-----	-----
C	(a)	.953	(a)	1.02
Nb-1%Zr	.925	.938	-----	-----
Mo	[b].596	[b].872	[b].656	[b].908
Hf	[b]1.04	[b].847	1.08	.899
Ta	[b].825	[b].786	[b].846	[b].808
W	[b].721	[b].952	.792	.946
Re	1.13	.849	-----	-----

[a]Negative absorptive correction factors.

[b]Iterated values.

Analysis of Critical Assemblies Using Corrected GAM II Cross Sections

Los Alamos critical assemblies. - Several Los Alamos critical assemblies (ref. 11) containing Oy, Ta, and Mo were reanalyzed using corrected GAM II cross sections. With unaltered GAM II cross sections, these assemblies were previously calculated to have a k_{eff} greater than unity although pure oralloy assemblies were calculated satisfactorily.

Molybdenum reflected oralloy: This critical assembly consists of a 13.33-centimeter (5.25-in.) diameter Oy cylinder (93.5 wt. % ^{235}U with a height to diameter ratio of 1.02). The density of the oralloy was 18.8 grams per cubic centimeter, and the critical mass was 35.0 kilograms. The core was reflected on all sides by 2.54 centimeters (1.0 in.) of 99.8-weight-percent molybdenum. A 0.819-cubic-centimeter (0.05-in.^{3}) central cavity that accommodated the neutron source was included in the calculations.

The calculations were made in 2D RZ using the DOT code with the P_0S_8 approximation and the 13-group structure given in table IV. The square root of the buckling in the spectrum calculation was taken as 0.3 reciprocal centimeter. Tape nuclide 42.000 was used to generate the spectrum averaged molybdenum cross sections.

For the base calculation, which used the unaltered GAM II cross-section set, the calculated eigenvalue was 1.03812. Applying the 13-group correction factors for molybdenum as given in table VII to the spectrum-averaged broad-group GAM II cross sections reduced the eigenvalue by 1.3 percent to 1.02427.

A previous calculation of this assembly yielded a base eigenvalue of 1.0285 when a P_1 approximation in the scattering expansion was used with a S_4 angular quadrature in 13 groups and an eigenvalue of 1.0248 for the case with a S_8 quadrature. Thus, it can be inferred that a P_1S_8 calculation of this critical assembly with corrected GAM II cross sections would yield an eigenvalue of 1.012.

Tantalum-oralloy core: A bare cylindrical critical experiment, 38.1 centimeters (15 in.) in diameter and 18.567 centimeters (7.31 in.) tall, containing 49.2-volume percent of oralloy and 50.8 volume percent tantalum was recalculated in P_0S_8 using a 13-group 2D RZ representation in the DOT code. The base eigenvalue was 1.0271, while the eigenvalue with the 13-group correction factors for tantalum given in table VII was 1.0090, a reduction of 1.74 percent. A previous calculation using 13 groups and a P_1S_4 approximation resulted in an eigenvalue of 1.029 for the base case, indicating the reduced importance of the P_1 approximation for this larger core. The S_4 to S_8 change has been shown to amount to about a -0.4 percent change in eigenvalue.

NCA composition number 1 critical assembly. - This core was the first of a series of critical configurations built to provide data to check the cross sections and analytical methods to be used on the heavy-metal-reflected, fast-spectrum reactor program. The critical assembly is shown in figure 1. Two-dimensional RZ calculations using 13 groups and a P_0S_4 approximation were made using a geometrical description similar to figure 12. The core contained only oralloy, tantalum, and a small amount of molybdenum. The core was reflected by a 8.26-centimeter (3.25-in.) radial reflector and a 10.2-centimeter (4.00-in.) axial reflector of molybdenum. The base case eigenvalue calculated using the unaltered cross section was 1.0242, and the corrected case eigenvalue was 1.007, a difference of 1.6 percent. The correction factors for 13 groups given in table VII for molybdenum and tantalum were used to correct the cross sections.

Error Analysis of the Cross-Section Correction Factors

Derivation of the error equations. - Equations (4) to (7) were solved for the spectrum-averaged cross-section correction factors A_m and S_m:

$$A_m = \frac{R_s M_c - M_E}{R_s C_c - C_E} \tag{13}$$

$$S_m = \frac{R_A M_c - M_E}{R_A C_c - C_E} \tag{14}$$

where

$$R_s = \frac{\int_{-L/2}^{L/2} C_s(R, z, m)dz}{\int_{-L/2}^{L/2} C_s(0, z, m)dz} = 1.48$$

$$R_A = \frac{\int_{-L/2}^{L/2} C_A(R, z, m)dz}{\int_{-L/2}^{L/2} C_A(0, z, m)dz} = 0.425$$

$$M_E = W_M(R, m)$$

$$M_c = W_M(0, m)$$

$$C_E = W_c(R, m)$$

and

$$C_c = W_c(0, m)$$

In the preceding equations R_s is the measured edge-to-center ratio of the specific integral worth for a scatterer, R_A is the measured edge-to-center ratio of the specific integral worth for an absorber, M_E is the measured edge worth for the sample m, M_c is the measured center worth for the sample m, C_E is the calculated edge worth for the sample m, and C_c is the calculated center worth for the sample m. (M_E, M_c, C_E, and C_c are in m¢/g.)

The error in A_m and S_m resulting from errors in the right hand side of equations (13) and (14) is then found by the procedure of propagation of errors to be

$$\left(\frac{\Delta A_m}{A_m}\right)^2 = \left(\frac{R_s M_c}{R_s M_c - M_E} - \frac{R_s C_c}{R_s C_c - C_E}\right)^2 \left(\frac{\Delta R_s}{R_s}\right)^2$$

$$+ \frac{1}{\left(R_s M_c - M_E\right)^2}\left[\left(R_s M_c\right)^2\left(\frac{\Delta M_c}{M_c}\right)^2 + M_E^2\left(\frac{\Delta M_E}{M_E}\right)^2\right]$$

$$+ \frac{1}{\left(R_s C_c - C_E\right)^2}\left[\left(R_s C_c\right)^2\left(\frac{\Delta C_c}{C_c}\right)^2 + C_E^2\left(\frac{\Delta C_E}{C_E}\right)^2\right] \qquad (15)$$

$$\left(\frac{\Delta S_m}{S_m}\right)^2 = \left(\frac{R_A M_c}{R_A M_c - M_E} - \frac{R_A C_c}{R_A C_c - C_E}\right)^2 \left(\frac{\Delta R_s}{R_s}\right)^2$$

$$+ \frac{1}{\left(R_A M_c - M_E\right)^2}\left[\left(R_A M_c\right)^2\left(\frac{\Delta M_c}{M_c}\right)^2 + M_E^2\left(\frac{\Delta M_E}{M_E}\right)^2\right]$$

$$+ \frac{1}{\left(R_A C_c - C_E\right)^2}\left[\left(R_A C_c\right)^2\left(\frac{\Delta C_c}{C_c}\right)^2 + C_E^2\left(\frac{\Delta C_E}{C_E}\right)^2\right] \qquad (16)$$

These error equations were used to compute the total error in the spectrum-averaged cross-section factors arising from (1) the uncertainty in the measured edge-to-center ratio of specific integral worths for two pure scatterers given in equation (2), (2) the uncertainty in the measured edge-to-center ratio of specific integral worths for two predominant absorbers, analytically corrected for scattering (eq. (3)), and (3) all the uncertainties in the quantities used to compute the cross-section correction factors. These uncertainties are listed on tables I and II.

Since $(R_s M_c - M_E)$ in equation (13) approaches zero for predominant scatterers, the error in A_m as developed in equation (15) is expected to be large for predominant scatterers. Similarly the error in S_m for predominant absorbers as given in equation (16) is large since the term $(R_A M_c - M_E)$ in equation (14) approaches zero.

These large errors do not, however, affect the capability of the correction factors to bring the calculated integral worths into agreement with the measurements. This is because for a predominant absorber the scattering cross section and, therefore, the error

in the scattering correction factor are unimportant in calculating the integral worth. Similarly, the absorption cross section and the error in the absorption correction factor is unimportant for a predominant scatterer.

Results of error analysis. - Table VIII presents the results of the error analysis for all the materials in terms of the total error. It is noted that for predominant scatterers such as C and Li the error in A_m is large and that for predominant absorbers such as ^6Li and B the error in S_m is large. For materials that are a balance between scattering and absorption, such as Nb-1 percent Zr, Mo, Hf, Ta, W, Re, the total error is less than 2 percent in the spectrum averaged correction factors.

As explained before, the measured values of the edge-to-center ratio for ^6Li and B, used to determine the value of R_A, were analytically corrected to account for scattering. A change in R_A affects only the value of S_m, the spectrum-averaged correction factor for scattering, as seen in equation (14). Also, S_m is insensitive to changes in R_A, since R_A appears in both the numerator and the denominator. Therefore, even if the analytical correction for scattering used in computing R_A were omitted, the value of S_m would change by less than 2 percent for Nb-1 percent Zr, Mo, Hf, Ta, and Mo; the materials of primary interest.

TABLE VIII. - ERROR ANALYSIS OF SPECTRUM-AVERAGED CROSS-SECTION CORRELATION FACTORS

Material, m	Four group		13 group	
	Absorptive correction factor, A_m	Scattering correction factor, S_m	Absorptive correction factor, A_m	Scattering correction factor, S_m
	Total error, %			
Li	3.1	4.1	2.8	3.9
^6Li	1.4	6.6	1.3	6.3
^7Li	220	4.5	220	4.9
$^7Li_3N$	17	3.4	-----	---
Be	13	4.3	-----	---
BeO	14	3.5	-----	---
$^{10}B/^{11}B$	1.4	8.6	1.4	8.7
^{10}B	1.8	9.3	-----	---
C	160	1.8	330	1.9
Nb-1%Zr	1.5	1.2	-----	---
Mo	1.8	1.3	1.9	1.3
Hf	1.2	1.2	1.2	1.2
Ta	1.1	1.1	1.1	1.1
W	1.2	1.1	1.1	1.1
Re	1.4	2.1	-----	---

CONCLUSIONS

A series of central and core-reflector interface material worth replacement experiments were performed in a fast-neutron spectrum reactor having negligible resolved resonance flux. The experiments were analyzed in four and 13 neutron groups using two-dimensional S_N transport theory programs. The method of Engle, Hansen, and Paxton, wherein the measured integral worth at various radii are separated into absorption and scattering components, was extended to apply to both measured and calculated integral worths thereby permitting the computation of spectrum-averaged cross section correction factors for the various materials.

It was found that the ratios of edge-to-central specific worths of pure scatterers and predominant absorbers were essentially constant over a useful range of cross-sections, independent of the particular material, showing the separability of scattering and absorptive effects. This conclusion was supported by calculation.

Since the extended method produces spectrum-averaged cross-section factors that are applied equally to all groups, it is unable to cope with uncertainties in the cross-section shape and the inelastic scattering model. However, the good agreement between (1) the four- and 13-group derived spectrum-averaged absorption cross-section correction factor for materials in which absorption was dominant, (2) the four- and 13-group spectrum-averaged scattering cross section for scattering materials, and (3) the general good agreement for materials that are mixtures of absorption and scattering showed that the effects of the cross-section shape on the value of the correction factor was secondary.

The cross-section correction factors computed for molybdenum and tantalum were in the direction and magnitude to bring the persistently overpredicted eigenvalue of the Los Alamos oralloy-molybdenum reflected and 49.2-percent Oy - 50.8-percent tantalum bare cores, and the NCA Composition 5A oralloy-tantalum-molybdenum core to within 1 percent of the experimental reactivity.

Lewis Research Center,
National Aeronautics and Space Administration,
Cleveland, Ohio, September 13, 1972,
503-25.

REFERENCES

1. Moore, R. A.; Sargis, D. A.; and Cohen, S. C.: Integral Tests of ENDF/B and GAM Neutron Cross-Section Data in a Clean Fast Assembly. Nucl. Sci. Eng., vol. 39, no. 2, Feb. 1970, pp. 263-272.

2. Engle, L. B.; Hansen, G. E.; and Paxton, H. C.: Reactivity Contributions of Various Materials in Topsy, Godiva, and Jezebel. Nucl. Sci. Eng., vol. 8, no. 6, Dec. 1960, pp. 543-569.

3. Joanau, G. D.; and Dudek, J. S.: GAM-II. A B_3 Code for the Calculation of Fast-Neutron Spectra and Associated Multigroup Constants. Rep. GA-4265, General Dynamics Corp., Sept. 16, 1963.

4. Mayo, Wendell; and Lantz, Edward: Analysis of Fuel Loading Requirements and Neutron Energy Spectrum of a Fast Spectrum, Molybdenum-Reflected, Critical Assembly. NASA TM X-52762, 1970.

5. Heneveld, W. H.; Paschall, H. R. K.; Springer, T. H.; Swanson, V. A.; Thiele, A. W.; and Tuttle, R. J.: Experimental Physics Characteristics of a Heavy-Metal-Reflected Fast-Spectrum Critical Assembly. Rep. AI-71-31, Atomics International (NASA CR-72820), July 30, 1971.

6. Heneveld, W. H.; et al: Summary Report No. II, Experimental Physics Characteristics of a Heavy-Metal-Reflected Fast-Spectrum Critical Assembly. NASA CR-120959, 1972.

7. Barber, Clayton E.: A FORTRAN IV Two-Dimensional Discrete Angular Segmentation Transport Program. NASA TN D-3573, 1966.

8. Mynatt, F. R.; Muckenthaler, F. J.; and Stevens, P. N.: Development of Two-Dimensional Discrete Ordinates Transport Theory for Radiation Shielding. Rep. CTC-INF-952, Union Carbide Corp. (AD-692168), Aug. 11, 1969.

9. Mayo, Wendell: Precritical Analysis of a Power-Tailored Fast-Spectrum Molybdenum Reflected Critical Assembly. NASA TM X-52895, 1970.

10. Anderson, John L.: PERTRAN - A Transport-Perturbation Program. NASA TN D-5906, 1970.

11. Paxton, H. C.: Los Alamos Critical-Mass Data. Rep. LAMS-3067, Los Alamos Scientific Lab., May 6, 1964.

12. Anderson, John L.; and Mayo, Wendell: Effect of Adding Lithium Nitride, Hafnium, Tantalum, and Tungsten to a Fast-Spectrum, Molybdenum-Reflected Critical Assembly. NASA TM X-52787, 1970.

NASA-Langley, 1972 — 22 E-7069